Numerical investigation of the seakeeping of a Flettner rotors-propelled catamaran in beam waves

Fabio Pili, Aurélien Babarit, Félicien Bonnefoy, Grégory S Payne

Numerical investigation of the seakeeping of a Flettner rotors-propelled catamaran in beam waves

Fabio Pili
Nantes Université, École Centrale Nantes, CNRS, LHEEA, UMR 6598, F-44000 Nantes, France. fabio.pili@ec-nantes.fr.

Aurélien Babarit
Nantes Université, École Centrale Nantes, CNRS, LHEEA, UMR 6598, F-44000 Nantes, France.

Félicien Bonnefoy
Nantes Université, École Centrale Nantes, CNRS, LHEEA, UMR 6598, F-44000 Nantes, France.

Grégory S. Payne
Farwind Energy, 44300 Nantes, France.

Abstract. This paper deals with the seakeeping of a catamaran propelled by Flettner rotors. The case study is a specific design of an energy ship. The prediction of the roll motion of such a ship is of particular interest since she will mostly sail in beam seas. We used a numerical model based on the boundary element method (BEM) to deal with the interactions of the ship with waves. It is supplemented by a model for the aerodynamic damping effect due to the rotors and by the ITTC correction for roll damping. In the present study, it has been assumed that the Flettner rotors can be modelled as a distribution of elementary airfoils whose lift and drag depend on the local apparent wind speed. Interaction effects between the rotors and between the hull and rotors have been neglected. Regular waves have been investigated. For the considered case study, it is found that the Flettner rotors have a small negative damping effect on the ship motion.

Keywords: Flettner rotor; Seakeeping; Roll Motion; Sail aerodynamics; Boundary Element Method; Energy ship

1 INTRODUCTION

Climate change is a significant threat to our societies. To prevent disastrous outcomes, the increase in global temperature must be kept below 2°C according to IPCC et al. (2018). It requires a drastic reduction in global greenhouse gas emissions, a goal which requires the development of new technologies including wind assisted ship propulsion (WASP) systems (soft sails, wingsails, Flettner rotors, kite, turbosails) and marine renewable energy (MRE) converters (offshore wind turbines, wave energy converters, tidal energy converters).

In this context, the company Farwind Energy was founded in 2020 in order to develop new systems for offshore wind energy harvesting (www.farwind-energy.com). Those systems are based on the energy ship technology (Salomon, 1982). An energy ship is a vessel propelled by the wind and equipped with hydroturbines so that electrical power is produced while sailing. The generated electricity is stored on board, either in batteries or through its conversion into fuel (hydrogen, ammonia, methanol, etc.). A key advantage of the energy ship is that it enables the harvesting of far offshore wind energy which, despite being the second greatest renewable energy source on the planet, is left largely unexploited to date. Examples of proposed energy ship concepts are described in Kim and Park (2010), Platzer et al. (2014), Ouchi and Henzie (2017), Gilloteaux and Babarit (2017).

Figure 1 shows a picture of an example energy ship design which has been proposed by Ecole Centrale de Nantes (Babarit et al., 2021). It consists of a catamaran vessel propelled by four Flettner

rotors. It is equipped with two hydroturbines attached underneath the hull. Further details of this design are provided in Table 1.

Table 1. Energy ship design specifications

Hull		
Length	m	80
Breadth	m	31.7
Draft	m	2.1
Displacement	t	31.7
Structural mass	t	560
Wind propulsion		
Type	-	Flettner rotors
Number	-	4
Rotor height	m	35
Rotor diameter	m	5
Rotor mass	t	79
Rotor drive power (max)	kW	143

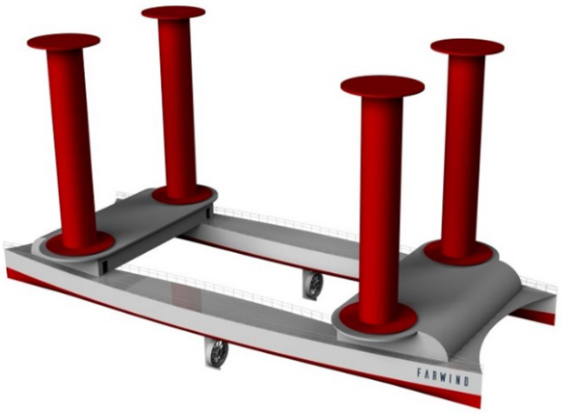

Figure 1. Artist's view of the energy ship design

According to Babarit et al. (2021), maximum power production is achieved when the ship is sailing beam wind. In practice, beam wind will very often correspond to beam sea conditions (as waves are generated by the wind). Therefore, it is critical to investigate in the early design phases whether wave-induced roll motion may be a challenge regarding the ship's safety and operability.

Several studies have been published in the scientific literature regarding the roll motion prediction of seagoing vessels. The basis equation of motion of ships and offshore structures in waves can be found in e.g. Faltinsen (1993). Ikeda (1978) conducted several studies to investigate the roll damping components of marine vessels. The outcome of his works was a set of empirical formulas for various roll damping components for mono-hulls and catamaran vessels, which are still recommended by ITTC (2011). Katayama et al. (2011) carried out experimental investigations on the roll damping characteristics of multi-hulls vessels, both with and without forward speed. It showed that the effect of forward speed on roll damping is significant for a catamaran, especially for low values of forced roll amplitudes at low Froude numbers ($F_n < 0.3$).

It is well known to the yachtsman that the roll of a yacht with its sails up is significantly smaller than that without the sails. The same effect has been reported for wind-assisted ships (Kuuskoski and V., 2023). Aerodynamic damping effects of wind propulsion devices including Flettner rotors were examined theoretically by F.M.Sinclair (1991). That work showed that if Flettner rotors operate at a

sufficiently high spin ratio (greater than 4), they have a stabilizing effect on roll motion. However, it was also observed that they can be destabilizing for apparent wind angles between 40° and 60 ° and spin ratio equal to 2. No data is available for other values of spin ratio. Copuroglu and Pesman (2018) investigated the effect of Flettner rotors on roll motion of a cargo ship case study using CFD (Lattice Boltzmann methods). It is found that the maximum roll angle is increased. However, results show that the increase is essentially due to the non-zero heel angle associated with the presence of the rotors. The effect of the rotors on the roll motion amplitude appears to be much smaller.

In this study, we investigate the effect of Flettner rotors on the roll motion of an energy ship. Firstly, the models of the Flettner rotor and of the ship are presented. Secondly, results of simulations based on those models are discussed.

2 MODEL

To predict the motions of the ship in the six degrees of freedom (DoF), let us define three coordinate systems (Figure 2):

- The Earth-fixed reference frame $(\mathbf{O}, \vec{x}_0, \vec{y}_0, \vec{z}_0)$ where $z = 0$ is the water surface at rest. This reference frame is oriented upwards.
- The manoeuvrability reference frame $(\mathbf{G}, \vec{x}_0, \vec{y}_0, \vec{z}_0)$ where $\mathbf{G}$ is the ship center of gravity. Its coordinates in the Earth-fixed reference frame are denoted (X, Y, Z).
- The Ship-fixed reference frame $(\mathbf{G}, \vec{x}_b, \vec{y}_b, \vec{z}_b)$. $\vec{x}_b$ is positive forward, $\vec{z}_b$ positive upwards and aligned with the rotor axis, $\vec{y}_b$ is oriented such that the reference frame is right-handed. Let φ be the roll angle, θ be the pitch angle and ψ be the yaw angle.

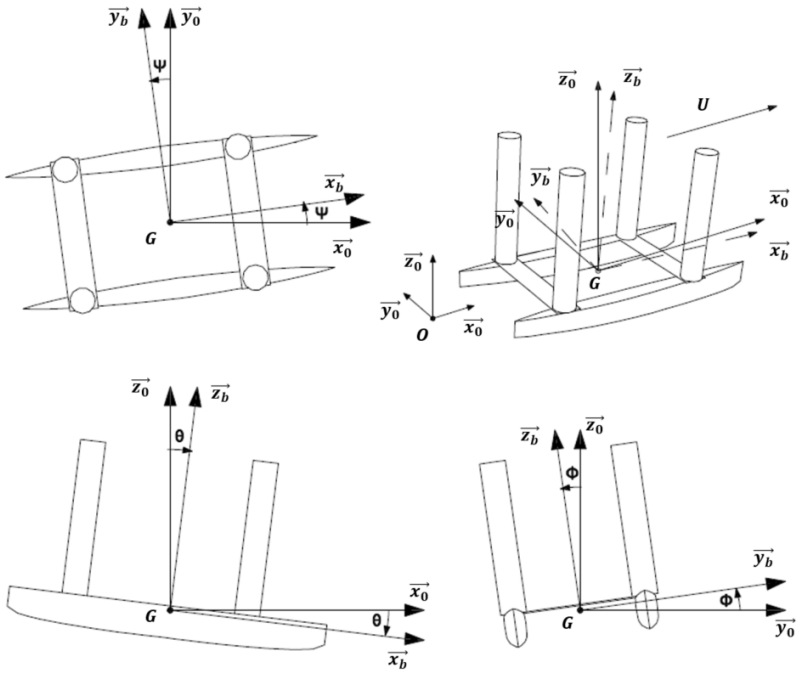

Figure 2. Seakeeping coordinate systems

2.1 Flettner rotor model

2.1.1 Aerodynamic force and aerodynamic damping matrix in quasi-static approach

In this study, the Flettner rotors are modelled as a distribution of elementary airfoils whose lift and drag depend on the local apparent wind speed. The aerodynamic interactions between the rotors have been neglected. The diameter and height of the rotor are denoted D and H respectively. The aerodynamic force $\mathbf{F}_a$ acting on a Flettner rotor can then be written:

$$\mathbf{F}_a = \int_{h=0}^{H} \frac{1}{2}\rho_a D V(h)^2 \begin{pmatrix} C_x(h) \\ C_y(h) \\ 0 \end{pmatrix}_b dh \tag{1}$$

where ρ_a is the air density, $V(h)$ is the apparent wind speed projected in the plane perpendicular to the rotor axis and passing by the point located at the distance h from the rotor bottom along the rotor axis (center of strip $\mathbf{P}(h)$ of the rotor), C_x is the thrust coefficient, C_y is the side force coefficient.

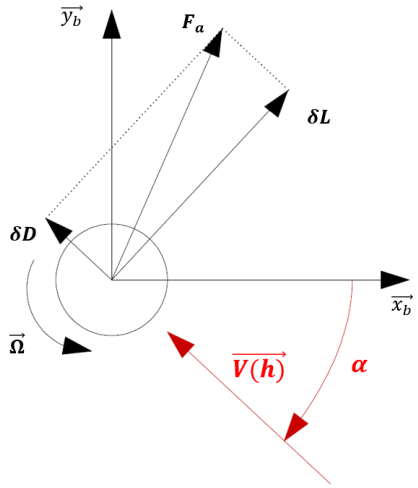

Figure 3. Flettner rotor force diagram

The local lift force δL , local drag force δD, thrust and side force coefficients are related to the local lift coefficient C_L and drag C_D coefficient (Figure 3):

$$\begin{aligned} C_x &= C_L \sin(\alpha) - C_D \cos(\alpha) \\ C_y &= C_L \cos(\alpha) + C_D \sin(\alpha) \\ \delta\mathbf{L}(h) &= \frac{1}{2}\rho_a C_L D V(h)^2 dh \\ \delta\mathbf{D}(h) &= \frac{1}{2}\rho_a C_D D V(h)^2 dh \end{aligned} \tag{2}$$

where α is the local apparent wind angle.

The apparent wind speed depends on the true wind speed and on the ship motion. Let $W(z)$ be the true wind speed and β the true wind angle. Let (χ_B, ξ_B, ζ_B) be the coordinates of the rotor bottom in the ship reference frame. Assuming that the ship rotations are small, one can show that the ship-induced velocity of point $\mathbf{P}$ along the rotor axis can be written:

$$\mathbf{U}(\mathbf{P}) = \begin{pmatrix} \dot{X} + (\zeta_B + h)\dot{\theta} - \xi_B\dot{\psi} \\ \dot{Y} + \chi_B\dot{\psi} - (\zeta_B + h)\dot{\varphi} \\ \dot{Z} + \xi_B\dot{\varphi} - \chi_B\dot{\theta} \end{pmatrix}_b \tag{3}$$

Therefore, the total apparent wind speed $\mathbf{V_T}$ is:

$$\begin{aligned}
&\mathbf{V_T}(\mathbf{P}) = \mathbf{W}(\mathbf{P}) - \mathbf{U}(\mathbf{P}) \\
&\mathbf{V_T}(\mathbf{P}) = \begin{pmatrix} -W(z)\cos(\beta+\psi) - \dot{X} - (\zeta_B + h)\dot{\theta} + \xi_B\dot{\psi} \\ W(z)\sin(\beta+\psi) - \dot{Y} - \chi_B\dot{\psi} + (\zeta_B + h)\dot{\varphi} \\ W(z)\theta\cos(\beta+\psi) + W(z)\varphi\sin(\beta+\psi) - \dot{Z} - \xi_B\dot{\varphi} + \chi\dot{\theta} \end{pmatrix}_b
\end{aligned} \tag{4}$$

The apparent wind speed projected in the plane perpendicular to the rotor $V(h)$ and the apparent wind angle α are thus given by:

$$\begin{cases} V(h)^2 = & \begin{pmatrix} \left(-W(z)\cos(\beta+\psi) - \dot{X} - (\zeta_B + h)\dot{\theta} + \xi_B\dot{\psi}\right)^2 + \\ \left(W(z)\sin(\beta+\psi) - \dot{Y} - \chi_B\dot{\psi} + (\zeta_B + h)\dot{\varphi}\right)^2 \end{pmatrix} \\ V(h)\cos\alpha = & W(z)\cos(\beta+\psi) + \dot{X} + (\zeta_B + h)\dot{\theta} - \xi_B\dot{\psi} \\ V(h)\sin\alpha = & W(z)\sin(\beta+\psi) - \dot{Y} - \chi_B\dot{\psi} + (\zeta_B + h)\dot{\varphi} \end{cases} \tag{5}$$

In Equation 4, the true wind speed depends on the vertical coordinate $z = Z - \chi_B\theta + \xi_B\varphi + \zeta_B + h$ to take into account the atmospheric boundary layer. This dependency can be modelled by:

$$W(\mathbf{z}) = W_r\left(\frac{z}{z_r}\right)^{\sigma} \tag{6}$$

where z_r is the reference height (usually 10 m) and σ is the Hellmann coefficient. According to Touma (1977) $\sigma = 0.11$ can be used for open water.

Let Ω be the rotor's rotational speed. Let $SR(h) = \Omega D/(2V(h))$ be the local spin ratio at height h along the rotor axis. According to Tillig and Ringsberg (2020), the lift and drag coefficients of the rotor C_L and C_D can be expressed as function of the spin ratio as:

$$\begin{aligned}
C_L =& 0.0046SR^5 + 0.11SR^4 - 0.98SR^3 + 3.1SR^2 - 0.10SR \\
C_D =& -0.0017SR^5 + 0.046SR^4 - 0.44SR^3 + 1.7SR^2 - 1.6SR + 0.64
\end{aligned} \tag{7}$$

Note that the lift and drag coefficients in Equation 7 are 2D coefficients that have been derived from CFD results of Li and Leer-Andersen (2012) and have been corrected to better match the full-scale measurements (see Tillig and Ringsberg, 2020). Those coefficients were applied to each strip of the rotors. The moment $\mathbf{M}_a$ at the bottom of the rotor $\mathbf{B}$ is:

$$\mathbf{M}_a(\mathbf{B}) = \int_{h=0}^{H} \frac{1}{2}\rho_a D V^2(h) \begin{pmatrix} -hC_y(h) \\ hC_x(h) \\ 0 \end{pmatrix}_b dh \tag{8}$$

Finally, let us define the aerodynamic damping matrix $\mathbf{B_a}$ by:

$$B_{a,ij} = \frac{\partial \tilde{F}_{a,i}}{\partial \dot{X}_j} \tag{9}$$

where $\tilde{\mathbf{F}}_\mathbf{a} = [\mathbf{F_a}, \mathbf{M_a}(\mathbf{G})]^T$ is the generalized aerodynamic force and $\mathbf{X} = [X, Y, Z, \varphi, \theta, \psi]^T$ is the ship motion. All the previous equations define what we consider the quasi-static model of the Flettner rotors for the example energy ship design shown in Figure 1.

2.1.2 Case of pure roll motion and linearization

In principle, the stabilizing effect of the rotor could be analyzed by assessing the eigenvalues of the aerodynamic damping matrix $\mathbf{B_a}$. However, its expression is too complex in the general case to perform such a task by hand. Moreover, in this study, the focus is on the effect of the rotors on roll motion. Therefore, in this section, let us assume that the ship is moving forward with constant speed ($\dot{X} = U$) and that it is moving only in roll ($\dot{Y} = \dot{Z} = 0$ and $\dot{\theta} = \dot{\psi} = 0$). The dependence of the true wind speed on the height is also neglected ($W(z) = W_{10}$) and the ship is supposed to sail beam wind ($\beta = 90^o$).

Recalling that the roll motion is supposed to be small, the apparent wind speed Equation 5 simplifies to:

$$\left\{ \begin{array}{rcl} V(h) & = & V_0 \left(1 + \frac{W_{10}}{V_0^2}(\zeta_B + h)\dot{\varphi}\right) \\ V(h)\cos\alpha & = & U \\ V(h)\sin\alpha & = & W_{10} + (\zeta_B + h)\dot{\varphi} \end{array} \right. \tag{10}$$

where $V_0^2 = W_{10}^2 + U^2$.

Let us recall that the aerodynamic moment along the x-axis of the ship at the bottom of the rotor is:

$$M_{a,x}(\mathbf{B}) = -\int_{h=0}^{H} \frac{1}{2}\rho_a D V(z)^2 h C_y dh \tag{11}$$

It can be rewritten:

$$M_{a,x}(\mathbf{B}) = -\int_{h=0}^{H} \frac{1}{2}\rho_a D h V(z)\, V(z) C_y dh \tag{12}$$

According to equations 2 and 10:

$$\begin{aligned} V(h)C_y(h) =& C_L(h)V(h)\cos(\alpha) + C_D(h)V(h)\sin(\alpha) \\ V(h)C_y(h) =& C_L(h)U + C_D(h)(W_{10} + (\zeta_B + h)\dot{\varphi}) \\ V(h)C_y(h) =& V_0 C_y(0) + \left(U\frac{\partial C_L}{\partial \dot{\varphi}}\Big|_{\dot{\varphi}=0} + (\zeta_B + h)C_D(0)\right)\dot{\varphi} + o(\dot{\varphi}) \end{aligned} \tag{13}$$

where the lift and drag coefficients have been replaced by their Taylor expansion at first order.

Using Equation 13 and Equation 10, one can show that the aerodynamic moment in roll can be written:

$$\begin{aligned} M_{a,x}(\mathbf{B}) =& M_{a,x,0}(\mathbf{B}) \\ & - \frac{1}{2}\rho_a D V_0 H^2 \left\{ \frac{U}{H^2}\int_{h=0}^{H} h\frac{\partial C_L}{\partial \dot{\varphi}}\Big|_{\dot{\varphi}=0} dh + (\frac{1}{2}\zeta_B + \frac{H}{3})(C_{D,i,0} + \frac{W_{10}}{V_0}C_{y,i,0}) \right\} \dot{\varphi} + o(\dot{\varphi}) \end{aligned} \tag{14}$$

By inspecting Equation 14, one can see that the aerodynamic moment induced by roll is stabilizing if:

$$\int_{h=0}^{H} h\frac{\partial C_L}{\partial \dot{\varphi}}\Big|_{\dot{\varphi}=0} dh > -\frac{H^2}{U}(\frac{1}{2}\zeta_B + \frac{H}{3})(C_{D,i,0} + \frac{W_{10}}{V_0}C_{y,i,0}) \tag{15}$$

Thus, let us consider the derivative of the lift coefficient with respect to $\dot{\varphi}$. One can write:

$$\frac{\partial C_L}{\partial \dot{\varphi}} = \frac{\partial C_L}{\partial SR}\frac{\partial SR}{\partial V}\frac{\partial V}{\partial \dot{\varphi}} \tag{16}$$

According to equations 7 and 10 and to the definition of the spin ratio:

$$\begin{aligned}\frac{\partial C_L}{\partial SR} =& 0.023SR^4 + 0.46SR^3 - 2.9SR^2 + 6.3SR - 0.10\\ \frac{\partial SR}{\partial V} =& -\frac{\omega D}{2V^2} = -\frac{SR}{V}\\ \frac{\partial V}{\partial \dot{\varphi}} =& \frac{W_{10}}{V_0}(\zeta_B + h)\end{aligned} \tag{17}$$

Thus, by combining equations 17 and Equation 15, one can show:

$$\begin{aligned}&\int_{h=0}^{H} h\frac{\partial C_L}{\partial \dot{\varphi}}\Big|_{\dot{\varphi}=0} dh =\\ &-\left(0.023{SR_0}^4 + 0.46{SR_0}^3 - 2.9{SR_0}^2 + 6.3SR_0 - 0.10\right)\frac{SR_0}{V_0}\frac{W_{10}}{V_0}(\zeta_B\frac{H^2}{2} + \frac{H^3}{3})\end{aligned} \tag{18}$$

Taking this relation into account, the stabilization condition 15 can be re-written:

$$\underbrace{0.023{SR_0}^5 + 0.46{SR_0}^4 - 2.9{SR_0}^3 + 6.3{SR_0}^2 - 0.10SR_0}_{\Gamma} < \underbrace{\frac{V_0^2}{UW_{10}}(C_{D,i,0} + \frac{W_{10}}{V_0}C_{y,i,0})}_{\Lambda} \tag{19}$$

In practice, the typical range of spin ratio of Flettner rotors is $SR \in [0, 5]$. Typical true wind velocity and ship velocity may be $W_{10} = 9$ m/s and $U = 9$ m/s. Figure 4 shows the stabilization condition as function of the spin ratio for these velocities. One can see that if SR $\in [0, \simeq 0.5] \cup [\simeq 1.5, \simeq 3.1]$ the Flettner rotor effect is stabilizing. However, if $SR \in [\simeq 0.5, \simeq 1.5]$ or if $SR > 3.1$, it is found to be destabilizing. Moreover, for $SR > 3.1$, the destabilizing effect increases with increasing spin ratio.

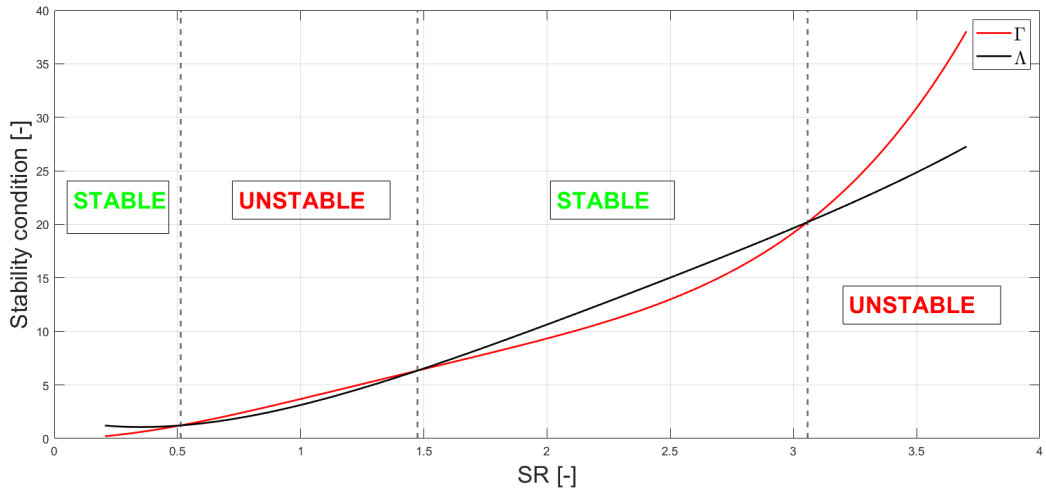

Figure 4. Stability condition for a single Flettner rotor in pure roll with W_{10}= 9 m/s and U=9 m/s

Our results disagree with that of F.M.Sinclair (1991). Indeed, according to her simulations, the effect is destabilizing for $SR = 2$ and stabilizing for $SR = 4$. The difference can be attributed to the lift and drag coefficients. Indeed, Sinclair used aerodynamic coefficients which were obtained through experiments (Clayton, 1985) carried out at $Re \approx 10^5$ whereas those used in the present study were derived from sea trials, corresponding to $Re > 10^6$. We re-ran the analysis with the same aerodynamic coefficients as those used by Sinclair (not shown in this paper for sake of brevity). In this case the

results better agree with hers: i.e destabilizing effect at low SRs and stabilizing effet at high SRs. However, the critical spin ratio for which the stability condition changes from a destabilizing effect to a stabilizing effect is $SR = 1.5$ (whereas it is between $SR = 2$ and $SR = 4$ in F.M.Sinclair (1991). That difference may be explained by the fact that she used a lifting line model in her study, which was not the case here.

2.2 Seakeeping model

The seakeeping model is based on the following equation of motion in regular waves:

$$[\mathbf{M} + \mathbf{A}(\omega_e)]\ddot{\mathbf{X}} + (\mathbf{B}(\omega_e) + \mathbf{B_{ITTC}}(\omega_e) + \mathbf{B_a})\dot{\mathbf{X}} + \mathbf{K}\mathbf{X} = A_s\mathbf{F}(\omega_e) \tag{20}$$

where we recall that $\mathbf{X}$ is the ship motion and $\mathbf{B_a}$ is the aerodynamic damping matrix, and where $\mathbf{A}$ is the added mass matrix, $\mathbf{B}$ is the radiation damping matrix, $\mathbf{F}$ is the excitation force transfer function, $\mathbf{B_{ITTC}}$ is the damping matrix correction suggested by ITTC (2011), $\mathbf{K}$ is the hydrostatic stiffness matrix and ω_e is the encounter frequency.

In this study, the BEM software NEMOH has been used (Babarit and Delhommeau, 2015) to calculate the hydrodynamic coefficients. Note that NEMOH does not take into account the forward velocity. Therefore, no corrections have been applied on the hydrodynamic coefficients.

The aerodynamic damping matrix $\mathbf{B_a}$ is derived from (9) using numerical differentiation. The damping matrix correction $\mathbf{B_{ITTC}}$ is computed as follows :

$$\mathbf{B_{ITTC}} = \mathbf{B_L} + \int_{x_0=-L_{PP}/2}^{L_{PP}/2} (\mathbf{B'_F} + \mathbf{B'_E})dx_0 + \int_{l=0}^{L_{SK}} \mathbf{B'_{SK0}}dl \tag{21}$$

Where $\mathbf{B_L}$, $\mathbf{B'_F}$, $\mathbf{B'_E}$ and $\mathbf{B'_{SK0}}$ are respectively the hull lift damping matrix, hull friction damping matrix per unit length, hull eddy damping matrix per unit length, and appendage damping matrix per unit length. In this study, the appendages are modelled as skegs. L_{SK} is the sum of the chord length of the appendages and L_{PP} is the boat length between its perpendiculars (in this case the waterline length). One can find in Table 2 the necessary data to compute the terms in equation (21) for the example energy ship design shown in Figure 1.

Table 2. Data used for the computation of the damping matrix B_{ITTC} (see ITTC (2011) for details)

Hull related terms	Unit	Value	Appendage related terms	Unit	Value
A_{HL}	m^2	336	l	m	17.5
V	m/s	9.00	L_{SK}	m	6.00
L_{PP}	m	80.0	b_{SK}	m	0.200
d	m	2.10	l_{sk}	m	8.00
l'_0	m	14.9	l_1	m	13.5
l'_r	m	15.2	l_2	m	1.54
$\bar{OG}$	m	14.6	l_3	m	0
b_{demi}	m	12.6	a	m^2	3.44

3 RESULTS

The models were implemented in a python script. The integrals in the rotor model were replaced by finite sums. The rotors were discretized in 25 elements which were found to be enough in practice to achieve convergence. In this study, we assumed $U = 9$ m/s, $W_{10} = 9$ m/s and $SR = 3.5$ corresponding to the nominal conditions for the energy ship design of Ecole Centrale de Nantes (Babarit et al., 2021).

3.1 Validity of the linear damping model

In order to investigate whether the linear damping model gives an acceptable approximation of the aerodynamic force, let us consider a single rotor in roll motion.

Figure 5 shows the aerodynamic moment variation $\Delta M_{a,x}(\mathbf{B})$ as function of the roll motion $\varphi(t) = A_\varphi \sin(\omega t)$ and the roll velocity $\dot{\varphi}(t) = A_\varphi \omega \cos(\omega t)$ computed using the quasi-static approach (Equation 8) and its linearization (Equation 14). The roll motion amplitude A_φ was set to 5° and 15°. Two periods $T = \frac{2\pi}{\omega}$ were considered : 5 s and 10 s. The combination of A_φ= 15 ° and T= 5 s is not considered for sake of brevity. For better understanding, the motion and velocities were expressed in degrees and degrees per seconds respectively for the first column.

Figure 5 shows that there are significant differences between the linear model and the quasi-steady state model. Even for the smallest motion amplitude and the longest period, the linear model overestimates the variation in aerodynamic moment by 26 %. Therefore, the linear model appears to be only a coarse approximation of the effect of motion on the aerodynamic force.

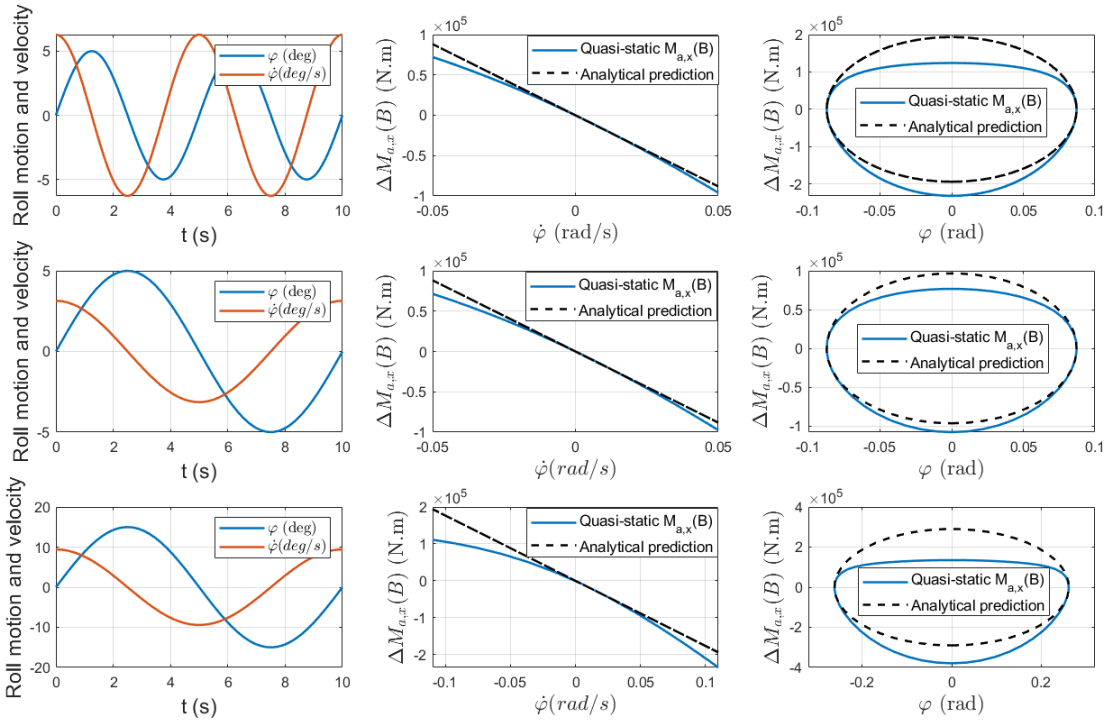

Figure 5. From left to right, forced roll angle and velocity, aerodynamic moment $\Delta M_{a,x}(\mathbf{B})$ and its linearization. First row for T= 5 s and A_φ= 5 °, second row for T= 10 s and A_φ= 5 °, third row for T=10 s and A_φ= 15 °. Computed for U =9 m/s, SR=3.5 and W_{10}= 9 m/s

3.2 Energy ship in regular waves

The RAOs of the proposed energy ship in beam waves were calculated according to Equation 20 and the linearized aerodynamic damping model (Equation 15) . The wave amplitude is 0.50 m for all wave frequencies. Note that aerodynamic interactions between the four rotors were neglected in this study.

Results are shown in Figure 6. The continuous blue curve corresponds to the predicted ship response with only wave radiation damping (aerodynamic damping and ITTC correction are neglected). The red curve with the round symbols shows the response with both aerodynamic and wave radiation damping. The dark yellow curve with the asterisk symbols shows the response with both ITTC and wave radiation damping. The dashed black curve shows the response with all damping sources. Note that the RAOs in surge, pitch and yaw are not shown since the response for these degrees of freedom is small compared to the others (less than 10^{-3} m/m or °/m).

Results show that for this particular ship design and wind/wave conditions, the Flettner rotors are destabilizing in roll. Indeed, taking into account aerodynamic damping increases the maximum roll angle by 6 % in comparison to that with only wave radiation damping (right panel in Figure 6). However, if the damping model including ITTC corrections for hull and appendages in addition to wave radiation damping is considered as a reference, one can see that taking into account aerodynamic damping leads to an increase of the maximum roll angle by 4 %. Therefore, the seakeeping behaviour of the energy ship design shown in Figure 1 appears to be not significantly affected by the Flettner rotors, at least for the considered operating conditions.

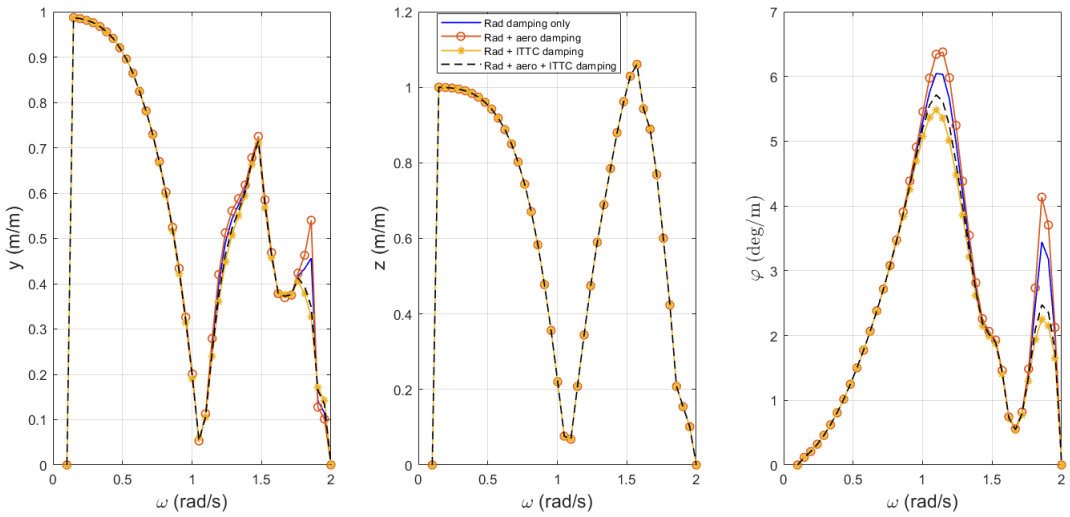

Figure 6. RAOs of the example energy ship in regular beam waves. The wave amplitude is 0.50 m for all wave frequencies. Other parameters are U_s= 9 m/s, β=90°, W_0= 9 m/s and SR=3.5

4 CONCLUSIONS

In this study, we investigated the effect of Flettner rotors on the seakeeping of an energy ship. The rotors were modelled using a quasi-static approach and a linearized approach in order to analyze the effect of the rotor in pure roll motion in beam seas. For a true wind speed and ship velocity of $W_{10} = 9$ m/s and $U = 9$ m/s it is shown that it can be stabilizing if SR $\in [0, \simeq 0.5] \cup [\simeq 1.5, \simeq 3.1]$. If $SR \in [\simeq 0.5, \simeq 1.5]$ or if $SR > 3.1$, the rotors are destabilizing.

The model was applied to take into account the effect of the rotors in seakeeping calculations. It is found that, for the case study in beam waves for $SR = 3.5$, the Flettner rotors have a small destabilizing effect in roll (no effect observed on the other degrees of freedom).

These preliminary results show that further research is needed on the effect of Flettner rotors on the seakeeping of energy ships. Indeed, comparisons between the linear model and the quasi-static model show that the accuracy of the linear model is rather limited even for small amplitude motion. Moreover, the model is based on several simplifications which may affect the conclusions. The strip-wise model of the rotor relies on 2D lift and drag coefficients which were calibrated based on experimental data for a particular rotor (Reynolds number, aspect ratio) on a particular ship (rotor-ship interactions). In the present study, even if the rotor geometry and operational regime are similar to those of the experiments, the rotor-ship interactions may be significantly different because of different ship geometries. Therefore, the 2D coefficients may actually be different for the ship considered in this study to that of the experimental data. Another likely highly significant simplification is that the aerodynamic interactions between the rotors were neglected.

The model is also based on a quasi-static approach. Possible missing dynamic effects are dynamic

stall and added mass. Gyroscopic effects were also not taken into account in the present analysis for sake of simplicity. It is believed that this assumption is acceptable because the rotational velocity of the rotors is an order of magnitude smaller than that it is required for anti-rolling gyros to stabilize ships. Nevertheless, this will have to be verified in future work.

Eventually, the seakeeping model used in the present study does not take into account the variation of the hull wetted surface. Indeed, when a catamaran experiences large roll motions, the hydrostatic stiffness matrix changes significantly (especially in the case of hull emergence) thus affecting significantly the prediction of his response to regular beam seas.

5 ACKNOWLEDGEMENTS

This work was supported by ANRT (French National Association for Research and Technology).

REFERENCES

Babarit, A. et al. (2021). “Exploitation of the far-offshore wind energy resource by fleets of energy ships – Part 2: Updated ship design and cost of energy estimate.” In: *Wind Energy Science* 6.5, pp. 1191–1204.

Babarit, Aurélien and Gérard Delhommeau (2015). “Theoretical and numerical aspects of the open source BEM solver NEMOH”. In: *Proc. of the 11th European Wave and Tidal Energy Conference (EWTEC2015)*. Nantes, France.

Clayton, B.R. (1985). “BWEA initiative on wind assisted ship propulsion”. In: *Proc. of the InternationalSymposium on Windship Technology (WINDTECH ’ 85)*. Southampton, U.K.: ASME.

Copuroglu, Hasan Islam and Emre Pesman (2018). “Analysis of Flettner Rotor ships in beam waves”. In: *Ocean Engineering* 150, pp. 352–362.

F.M.Sinclair (1991). *The motion damping characteristics of wind energy devices*. London: University College London.

Faltinsen, O (1993). *Sea Loads on Ships and Offshore Structures*. Cambridge: Cambridge University Press.

Gilloteaux, Jean-Christophe and Aurelien Babarit (2017). “Preliminary design of a wind driven vessel dedicated to hydrogen production”. In: *Proc. of the International Conference on Ocean, Offshore Mechanics and Artic Engineering*. Trondheim, Norway: ASME.

Ikeda, Yoshiho (1978). “Components of roll damping of ship at forward speed”. jap. In: ed. by Departement of Naval Architecture University of Osaka Prefacture. Berlin-Boston: Journal of Society of Naval Architects of Japan, pp. 21–54.

IPCC et al. (Dec. 2018). *Global warming of 1.5°C. An IPCC Special Report on the impacts of global warming of 1.5°C above pre-industrial levels and related global greenhouse gas emission pathways, in the context of strengthening the global response to the threat of climate change, sustainable development, and efforts to eradicate poverty*.

ITTC (2011). “Numerical estimation of roll damping.” In: *ITTC-Recommended procedures*. Gosport,UK: 6th ITTC Specialist Committee on Stability in Waves, pp. 7.5-02-07–04.5.

Katayama, Toru, Masanori Kotaki, and Yoshiho Ikeda (2011). “A Study on the Characteristics of Roll Damping of Multi-Hull Vessels”. In: vol. 97, pp. 487–498.

Kim, J. and C. Park (2010). “Wind power generation with a parawing on ships, a proposal”. In: *Energy* 35, pp. 1425–1432.

Kuuskoski, J. and Paakkari V. (2023). “Building trust in thrust”. In: *Proc. of the Wind Propulsion conference*. London,UK: The Royal Institution of Naval Architects, pp. 25–31.

Li, D. and B. Leer-Andersen M. Allenström (2012). “Performance and vortex formation of Flettner rotors at high Reynolds numbers”. In: *29th international Symposium on Naval Hydrodynamics*. Gottenburg.

Ouchi, K. and J. Henzie (2017). “Hydrogen generation sailing ship: conceptual design and feasibility study”. In: *In Proc. of the OCEANS conference*. Institute of Electrical and Electronics Engineers.

Platzer, Maximilian et al. (2014). “Renewable energy production using sailing ships”. In: *ASME Journal of Energy Resources Technology* 136.

Salomon, R.E. (1982). *Process of converting wind energy to elemental hydrogen and apparatus therefore*. U.S. Patent 4335093A.

Tillig, Fabian and Jonas W. Ringsberg (2020). “Design, operation and analysis of wind-assisted cargo ships.” In: *Ocean Engineering* 211.Number, p. 107603.

Touma, Jawad S. (1977). “Dependence of the Wind Profile Power Law on Stability for Various Locations”. In: *Journal of the Air Pollution Control Association* 27, pp. 863–866.